Study of Preparation and Properties on Polymer-modified Magnetite Nanoparticles

Ruili Tong[a,b], Yonggang Wang[a], Guang Yang[c], Aiqing Ma[d], Keji Sun[d], Hui Yang[b,*] and Jinben Wang[b]

[a]*School of Chemical and Environmental Engineering, China University of Mining and Technology (Beijing), Beijing 100083, People's Republic of China.*
[b]*Key Laboratory of Colloid, Interface and Chemical Thermodynamics, Institute of Chemistry, Chinese Academy of Science, Beijing 100190, People's Republic of China.*
[c]*CNOOC Research Institute, State Key Laboratory of Offshore Oil Exploitation, Beijing 100027, People's Republic of China.*
[d]*Oil Production Technology Research Institute, Shengli Oilfield Branch Company, Sinopec, Dongying, Shandong 257000, People's Republic of China.*

Received 17 June 2014, revised 4 March 2015, accepted 1 April 2015.

ABSTRACT

In this paper, polyacrylamide (PAM)-modified magnetite (Fe_3O_4) nanoparticles were prepared by *in situ* polymerization in aqueous solution. The particle size, morphology, crystal phase and magnetic properties were measured utilizing scanning electron microscopy (SEM), transmission electron microscopy (TEM), Fourier-transform infrared spectroscopy (FTIR), X-ray diffraction (XRD) and vibrating sample magnetometer (VSM), respectively. The size distribution and stability of the nanoparticles in aqueous solution were evaluated using the laser particle size analyzer and ultraviolet-visible spectroscopy (UV-vis). The influences of the dose of acrylamide (AM) and the pH value on the particle size and stability were also examined. The results showed that the Fe_3O_4 nanoparticles possessed superparamagnetic property and super dispersion stability in aqueous solution after PAM modification.

KEYWORDS

Magnetite (Fe_3O_4), nanoparticles, superparamagnetism, polymer modification, colloidal stability.

1. Introduction

Magnetic nanoparticles have attracted much more attentions for its wide-ranging application, including magnetic fluids, catalysis, biotechnology, data storage and environmental protection.[1–5] Amongst various magnetic nanoparticles, Fe_3O_4 nanoparticles have been recognized as a promising candidate for its good biocompatibility, strong superparamagnetism, low toxicity and easy preparation process.[6,7] However, pure Fe_3O_4 nanoparticles are likely to aggregate for their large specific surface area and strong magnetic dipole–dipole attractions between nanoparticles, resulting in aggregation in aqueous solution and the change of magnetic properties which should be avoided in applications.[8]

To avoid the aggregation of pure Fe_3O_4 nanoparticles during the application processes as mentioned above, modification on the surface of Fe_3O_4 nanoparticles with a surfactant or hydrophilic polymer is one of the most effective methods.[9,10] Furthermore, another significant function of the modification on the nanoparitcles is that the polymer or surfactant provides chemical groups for further grafting to satisfy further applications.[11]

Many researchers have discussed the modification of magnetic nanoparitcles. Yang *et al*. reported that the iron oxide nanoparticles were modified by various poly(amino acid)s for use as magnetic resonance probes.[12] Yu *et al.* investigated the hydroxypropyl-β-cyclodextrin/polyethylene glycol 400 modified on Fe_3O_4 nanoparticles for congo red removal.[13] Cui *et al*. studied perfluoropolyether carboxylic acid surfactant modified Fe_3O_4 magnetic nanoparticles and the modified layer could withstand high temperature.[14] Wang *et al.* presented modified magnetic nanoparticles using 3-aminopropyltriethoxy silane and subsequently activated by glutaraldehyde and then proteins were immobilized on the activated nanoparticles.[15] Several other materials were also reported on the modification of magnetic nanoparticles. For example, some reports confirmed that magnetic nanoparticles were coated by chitosan for applications in biotechnology.[16–18] Oleic acid was used to modify the surface of magnetite nanoparticles.[19,20] PEG/PVA and Poly(4-MS-DVB-GMA) matrix grafted with poly(amidoamine) PAMAM dendrimer were also suggested to modify magnetic nanoparticles.[21,22]

However, few studies on the modification of polyacrylamide (PAM) on the surface of magnetite nanoparticles appear in literature. PAM can be utilized to protect the particles' original properties and stabilize them in aqueous solution. In addition, this kind of magnetic composite can be moved effectively and simply by using applied magnetic field. In this paper, we prepared PAM-modified Fe_3O_4 nanoparticles *via* direct polymerization using the frequently-used bottom-up approach which was reported previously.[23–26] The Fe_3O_4 nanoparticles filler was encapsulated before and during the synthesis of the polymer.[27] The particle size distribution and the morphology of PAM-modified Fe_3O_4 nanoparticles were investigated. Other properties, such as crystal phase, magnetic properties and the mass lost value in TGA were also determined. Most importantly, the ζ-potential and stability of the PAM-modified nanoparticles in aqueous solution were illustrated.

2. Experimental

2.1. Materials

The chemicals used in this work were all analytical reagents. Ferric chloride ($FeCl_3$) was purchased from Sinopharm Chemical Reagent Beijing Co., Ltd., iron dichloride tetrahydrate ($FeCl_2{\cdot}4H_2O$) from Shanghai Gongxuetuan No. 2 Experiment

* To whom correspondence should be addressed. E-mail: yanghui@iccas.ac.cn

ISSN 0379-4350 Online / ©2015 South African Chemical Institute / http://saci.co.za/journal
DOI: http://dx.doi.org/10.17159/0379-4350/2015/v68a15

Factory, NaOH from Beijing Chemical Works, potassium persulfate ($K_2S_2O_8$) and acrylamide (AM) from Beijing Yili Fine Chemicals Co., Ltd.

2.2. Preparation of Fe_3O_4 Nanoparticles

3.25 g of $FeCl_3$ and 3.38 g of $FeCl_2 \cdot 10H_2O$ were successively dissolved in the 25 mL of deoxygenated water, which was obtained by bubbling nitrogen gas for 15 min, and then the solution was stirred and filtrated. The resulted solution was added dropwise into 200 mL of 1 M NaOH solution under vigorous stirring (600 r min^{-1}) under N_2 atmosphere, followed by the generation of Fe_3O_4 precipitate.

The total precipitate was isolated using a magnetic field, and the supernatant was removed by decantation. Then the precipitate was washed using purified deoxygenated water for several times with the same method, until no more Cl^- was detected upon addition of Ag^+. Finally, purified deoxygenated water was added to 1.7 g Fe_3O_4 precipitate until the total volume was 100 mL to form the required solution.

2.3. Preparation of Polymer-modified Magnetite Nanoparticles

The polymer modified magnetite nanoparticles were formed by bottom-up approach.[27] First, another 100 mL purified water was added to the Fe_3O_4 suspension prepared previously, to give 200 ml solution. Subsequently, 0.02 mol % of $K_2S_2O_8$ was added as initiator. After 10 minutes of ultrasonic vibration, AM (34 % by weight) solution was added dropwise into the above 200 mL of mixed solution under stirring (600 r min^{-1}) and ultrasonic vibration during the whole process. The solution was kept under N_2 atmosphere during the whole process.

Three kinds of products with different ratio of nanoparticles to AM were prepared, namely, PAM+10%Fe_3O_4, PAM+20%Fe_3O_4, PAM+50%Fe_3O_4. The pure Fe_3O_4 nanoparticles were also prepared for contrast. After polymerization, the samples PAM+10%Fe_3O_4 and PAM+20%Fe_3O_4 were semi-liquid jelly and dried in electric blast drying oven. For sample PAM+50%Fe_3O_4, the product was liquid, it was lyophilized. All the dried samples could be dispersed into water to form a homogeneous, transparent colloid. The results are summarized in Table 1.

2.4. Characterization

The sample phases and particle sizes were determined by X-ray diffraction (XRD) (Rigaku-D/max-2500, Japan). The morphology of the Fe_3O_4 Particles, before and after coated by PAM, were measured *via* micrographs obtained by scanning Electron Microscopy (SEM) (JSM-6700 JEOL, Japan) and transmission electron microscopy (TEM) (TECNAI-12, Philip Apparatus Co., USA). The size distribution and the stability of the PAM modified nanoparticles in aqueous solution were measured with a laser particle size analyzer (Horiba LB-550, Japan) and ultraviolet-visible spectroscopy (UV-vis) (UV2102, UNICO USA), respectively.

The infrared measurements in the 4000–400 cm^{-1} range on powder specimens dispersed on a pressed KBr disk, using a Fourier-transform infrared spectroscopy (FTIR) (Tensor27, Bruker Germany). The magnetic properties were carried out using a vibrating sample magnetometer (VSM) (MPMSXL, Quantum Design USA). The composition particles were also determined with thermogravimetric analysis (TGA) (Pyris 1, PerkinElmer USA).

3. Results and Discussion

3.1. Electron Microscopy

Figure 1 shows SEM and TEM images of the Fe_3O_4 particles before and after modification. The pure Fe_3O_4 particles are nearly spherical and have uniform morphology with the diameter about 10 nm. After modification, the particles became larger and the size varies from 30 to 100 nm. Particularly, the TEM image (b-2) shows that the particle is separated from its neighbours and the boundary is very clear.

3.2. X-ray Diffraction

Diffraction patterns of the samples (pure Fe_3O_4, PAM+10% Fe_3O_4, PAM+20%Fe_3O_4, PAM+50%Fe_3O_4) are shown in Fig. 2. The characteristic peaks of Fe_3O_4 cubic space group (2θ = 35.4 °, 62.74 °, 56.98 °, 30.34 °, 43.12 ° and 53.46 °) were observed. It is consistent with the standard pattern for Fe_3O_4 (JCPDS 19-629).[4,28,29] The average particle size calculated from the Debye-Scherrer formula is 9 nm, which is consistent with SEM/TEM results.

Compared to the pure Fe_3O_4, the characteristic peaks of the PAM-modified Fe_3O_4 particles are weak, but the position does not shift, which indicate that the PAM modified on the surface of the Fe_3O_4 particles does not change the size and crystal phase of the Fe_3O_4.

3.3. IR Results

The IR spectrum of the four samples is shown in Fig. 3. The peak near 574 cm^{-1} of the pure Fe_3O_4 curve belongs to the characteristic absorption band of the Fe-O bond,[4,7,30] and the absorption bands near 1632 cm^{-1} and 3418 cm^{-1} refers to the O-H stretching mode and H-O-H bending mode, indicating the presence of interstitial water in the samples.[7,28]

In the absorption curves of PAM-modified Fe_3O_4 nanoparticles, the 3450 cm^{-1} peak belongs to H–O bond vibrations of water,[3,28] and 3139 cm^{-1} peak belongs to N-H stretching vibrations.[23] 2783–2986 cm^{-1} can be assigned to the stretch vibrations of the C–H bonds which originates from the PAM modified on the surface of the particles.[3,28] The absorption bands near 1655 cm^{-1} shows common characteristic of $(NH_2)C{=}O$[23] and 1420 cm^{-1} represents the stretching vibration of the CN group.[30] In addition, the characteristic absorption band of Fe-O (around 580 cm^{-1}) still can be found in the PAM modified Fe_3O_4 nanoparticles.[28,30] Both of the absorption peaks from the PAM and Fe_3O_4 indicates that the magnetite nanoparticles have been well modified.

3.4. Magnetic Measurement

In order to investigate the magnetic properties of the samples, VSM was employed. Figure 4 shows the magnetization curves of samples at ambient temperature. Measurable hysteresis or

Table 1 Quality ratio of AM to Fe_3O_4 and dry methods.

Sample	Fe_3O_4/g	AM/g	Fe_3O_4: AM (by weight)	Drying method
PAM+50%Fe_3O_4	1.7	3.4	1:2	Freeze and vacuum
PAM+20%Fe_3O_4	1.7	8.5	1:5	Drying oven
PAM+10%Fe_3O_4	1.7	17	1:10	Drying oven

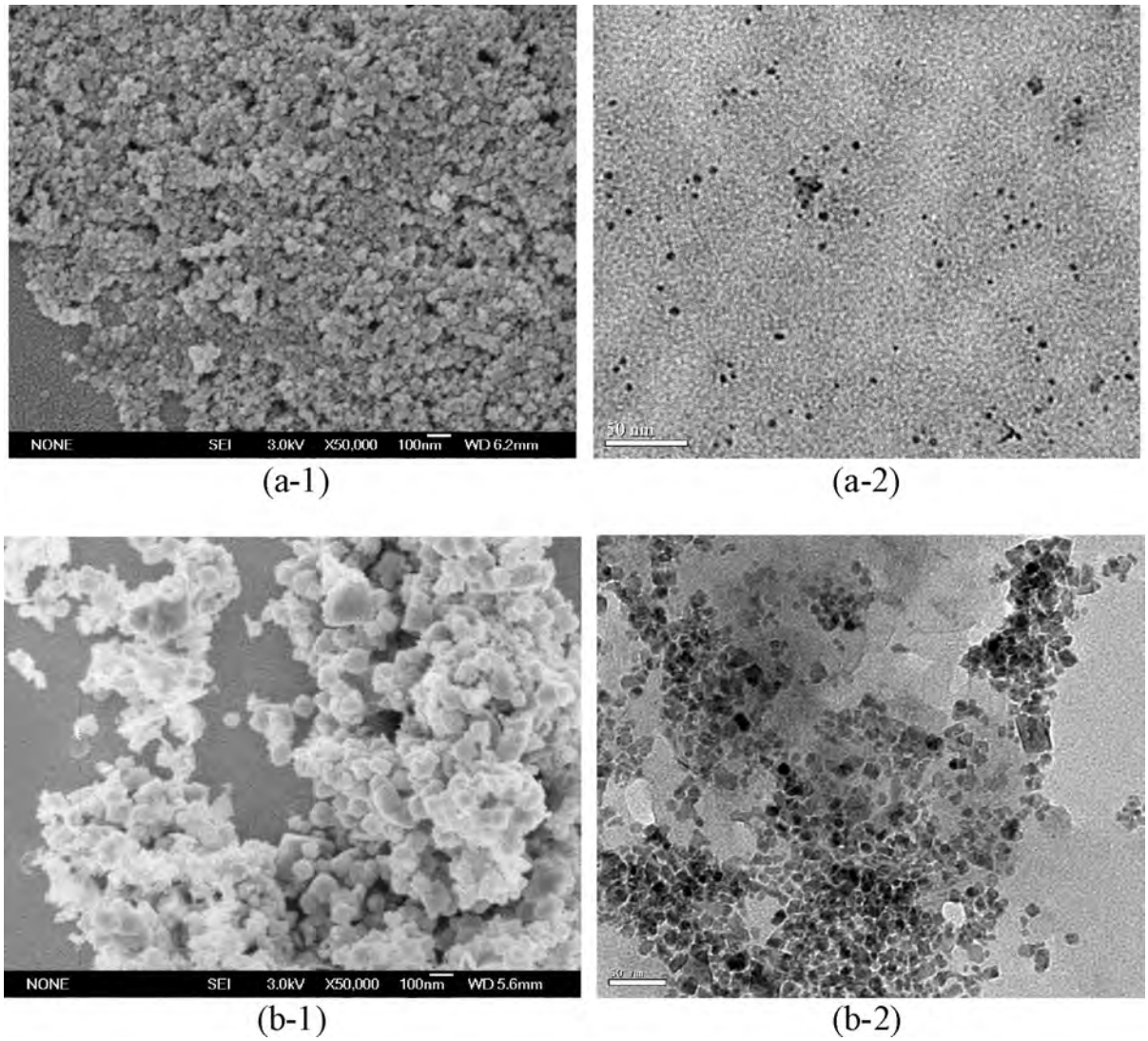

Figure 1 SEM and TEM for the Fe_3O_4 nanoparticles before (**a-1**, **a-2**) and after (**b-1**, **b-2**) polymer modification. (a-1: SEM; a-2: TEM; b-1:SEM; b-2:TEM).

coercivity were not observed in magnetization curves, indicating that all the samples show typical superparamagnetic behaviour.[8] The superparamagnetic behaviour also indicates that the particles' size range below 20 nm,[31] which is consistent with the morphological characteristics from the SEM/TEM in Fig. 1. The saturation magnetization was reached at a field of approximately 50 000 Oe. Figure 4 shows that the saturation measurements of the pure and PAM-modified Fe_3O_4 samples are approximately 53.5, 20.7, 7.9, 4.3 emu g^{-1}, respectively. The saturation magnetization of the nanoparticles is significantly smaller than that of bulk magnetite which is 84 emu g^{-1}.[8] It is believed that the decrease of measured saturation magnetization can be attributed to the reduction of size and the PAM coating.[1,7,8,12]

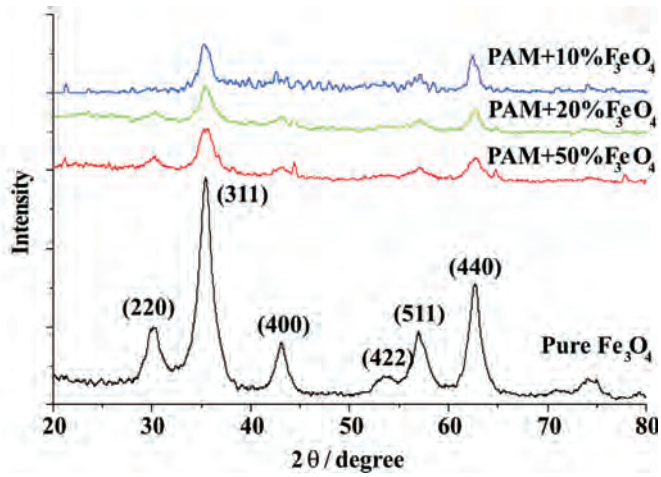

Figure 2 XRD patterns of pure and PAM-modified Fe_3O_4 nanoparticles.

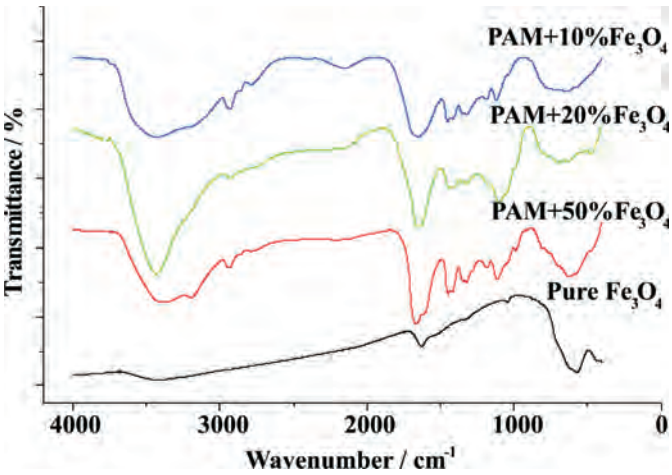

Figure 3 FTIR spectra of pure and PAM-modified Fe_3O_4 nanoparticles.

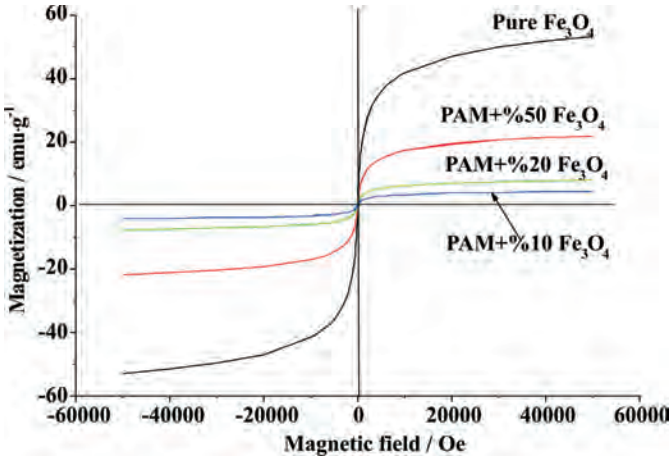

Figure 4 Magnetization curves of pure and PAM-modified Fe_3O_4 nanoparticles.

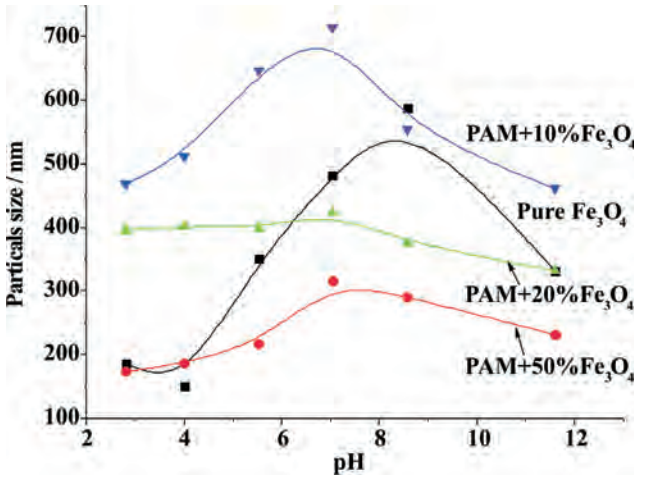

Figure 6 The influence of pH value on the size distribution of the nanaoparticles.

3.5. TGA

Four dried samples were subjected to TGA in the 30–650 °C range under an N_2 atmosphere (shown in Fig. 5). The pure Fe_3O_4 lost 13.3 % of its total weight, which is probably due to the absorbed water from the environment.[8] The PAM-modified samples show that there are three stages of mass loss for the thermal degradation of PAM. The first stage involves a slight weight loss around 9 % at temperature below 250 °C. It can be attributed to the presence water absorbed in PAM-modified Fe_3O_4 nanoparticles.[23] The second stage appears in the range of 250–380 °C for the decomposition of pendant amide groups and the intactness of polymer main chains.[23] The observed values of weight loss are around 24.5 %, 34.5 %, and 39.7 % for the three samples, respectively. The third stage appears in the range of 380–510 °C with 8 %, 10 %, and 11.5 % of weight loss for the different samples, respectively, due to the breakdown of the polymer backbones.[23]

3.6. The Aggregation of PAM-modified Nanoparticles in Aqueous at Different pH Values

The aggregation variety of the nanoparticles dispersed in water under different pH values are shown in Fig. 6. For pure Fe_3O_4 nanoparticles, at low pH value, the particles size is about 150 nm. As the pH rises, the aggregation becomes significant, for the size of the aggregate becomes larger and the maximum is up to 550 nm and after which the aggregation decreases as the pH value continues to rise. For the polymer-modified Fe_3O_4 nanoparticles, however, the slope of the aggregation curve is much more flat which means that polymer modified on the surface of Fe_3O_4 nanoparticles can effectively decrease their sensitiveness to pH. In order determine the principles involved for this phenomenon, the ζ--potentials of samples at different pH values were studied.

Figure 7 shows the relationship between the pH and the ζ-potential of pure and PAM-modified Fe_3O_4 nanoparticles. For pure Fe_3O_4 nanoparticles, at low pH value, the surface charge of the particles is initially positive (more than 40 mV) at pH~4. As a result, the particles aggregate less (shown in Fig. 6) due to the repulsive Coulombic force. At an intermediate pH value near the isoelectric point (IEP), where the surface charge density of particles is very low, the aggregation of magnetite particles becomes significant (shown in Fig. 6) due to the attractiveness of Van der Waals force.[32,33] At higher pH value far from the IEP, the overall charge is reversed and the repulsive Coulombic interactions among negative charged particles could again minimize the aggregation. So the ζ-potential of nanoparticle plays a vital role in aggregation of nanoparticles. But after modification of the particles with PAM, Fig. 7 shows that the nanoparticles' ζ-potential distribution is quite narrow which indicating that the ζ-potential of nanoparticles is not sensitive to the pH value.

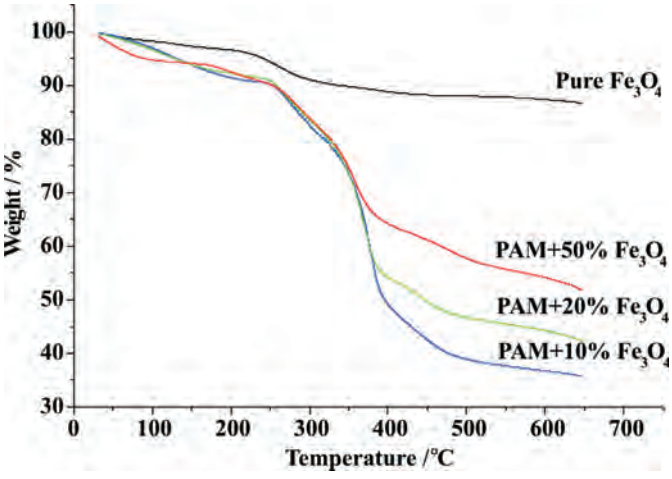

Figure 5 TG curves of pure Fe_3O_4 and PAM-modified Fe_3O_4 nanoparticles.

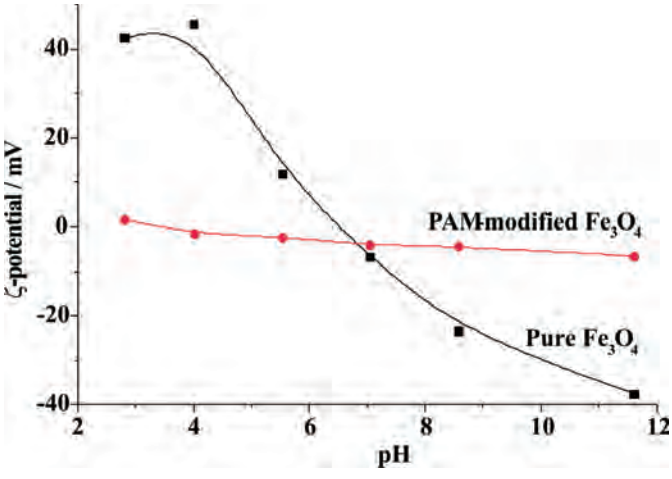

Figure 7 The ζ-potentials of the suspension at different pHs.

Aggregation of PAM-modified Fe_3O_4 nanoparticles at different pH is not as significant as the case for the pure Fe_3O_4 (shown in Fig. 6).

3.7. The Stability of the PAM-modified Nanoparticles in Water

The suspension stability in water of the pure and PAM-modified Fe_3O_4 was also studied using UV-vis measurement, as the aggregation and deposition rates can be reflected by the intension of UV-vis absorbance.[31,34] Figure 8 shows the absorbance intensity of the four samples, which were measured at different retention times. The absorbance of the pure Fe_3O_4 nanoparticles decreased sharply in the first hour and nearly becomes zero after 72 hours, which indicated that the pure Fe_3O_4 is not stable in the water and prone to aggregation and precipitation due high electromagnetic attractive forces between pure Fe_3O_4 nanoparticles. But after modification by the PAM, the absorbance intensity decreased only slightly after 72 hours, which indicates that PAM largely improves the stability of the nanoparticles in water. It can be attributed to the water-soluble PAM molecular chains that surround the particles and form a hydration shell to prevent them from aggregation and precipitation.

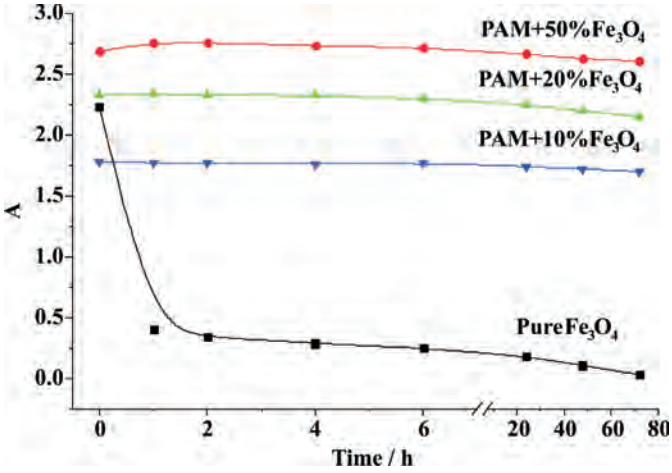

Figure 8 Time dependence of optical absorbance. (pH = 7.86, λ = 380 nm)

4. Conclusions

In this paper, the PAM modified superparamagnetic Fe_3O_4 nanoparticles were prepared. SEM shows that the single particle size is about 10–25 nm. XRD spectrum indicates that the produced nanoparticles are consistent with the standard pattern for Fe_3O_4. In addition, the FTIR spectrum demonstrated that PAM completely coated the surface of Fe_3O_4 nanoparticles. The magnetic measurement proves that the nanoparticles show superparamagnetic property. The absorbance intensity of UV-vis implies that the suspension stability of the nanoparticles in aqueous solution can be remarkably improved after being modified by PAM.

Acknowledgements

The authors are grateful to the Second Batch of Open Projects Funding from the State Key Laboratory of Offshore Oil Exploitation (CCL2013RCPS0244GNN) and the Important National Science and Technology Specific Project of China (2011ZX05024-004-03).

References

1 B. Kaboudin and A. Ghaderian, A novel magneto-fluorescent microsphere: preparation and characterization of polystyrene-supported Fe_3O_4 and CdS nanoparticles, *Appl. Surf. Sci.*, 2013, **282**, 396–399.
2 S. Zhang, F. Ren, W. Wu, J. Zhou, L. Sun, X. Xiao and C. Jiang, Size effects of Ag nanaoparticles on plasmon-induced enhancement of photocatalysis of Ag-α-Fe_2O_3 nanocomposites, *J. Colloid Interface Sci.* , 2014, **427**, 29–34.
3 N. Wu, L. Fu, M. Su, M. Aslam, K.C. Wong and V.P. Dravid, Interaction of fatty acid monolayers with cobalt nanoparticles, *Nano Lett.*, 2004, **4**, 383–386.
4 M.N. Esfahani, S.J. Hoseini, M. Montazerozohori, R. Mehrabi and H. Nasrabadi, Magnetic Fe_3O_4 nanoparticles: efficient and recoverable nanocatalyst for the synthesis of polyhydroquinolines and Hantzsch 1, 4-dihydropyridines under solvent-free conditions, *J. Mol. Catal. A: Chem.*, 2014, **382**, 99–105.
5 Y. Liu, Y. Chi, S. Shan, J. Yin, J. Luo and C. Zhong, Characterization of magnetic NiFe nanoparticles with controlled bimetallic composition, *J. Alloys Comp.*, 2014, **587**, 260–266.
6 H. Qin, C.M. Wang, Q.Q. Dong, L. Zhang, X. Zhang, Z.Y. Ma and Q.R. Han, Preparation and characterization of magnetic Fe_3O_4 – chitosan nanoparticles loaded with isoniazid, *J. Magn. Magn. Mater.*, 2015, **381**, 120–126.
7 G. Zhao, J. Feng, Q. Zhang, S. Li and H. Chen, Synthesis and characterization of prussian blue modified magnetite nanoparticles and its application to the electrocatalytic reduction of H_2O_2, *Chem. Mater.*, 2005, **17**, 3154–3159.
8 H. Shang, Wo. Chang, S. Kan, S. A. Majetich and G.U. Lee, Synthesis and characterization of paramagnetic microparticles through emulsion-templated free radical polymerization, *Langmuir*, 2006, **22**, 2516–2522.
9 S. Buendia, G. Cabanas, G. Alvarez-Lucio, H. Montiel-Sanchez, M.E. Navarro-Clemente and M. Corea, Preparation of magnetic polymer particles with nanoparticles of Fe(0), *J. Colloid Interface Sci.*, 2011, **354**,139–143.
10 M.Z. Rong, M.Q. Zhang, H.B. Wang and H.M. Zeng, Surface modification of magnetic metal nanoparticles through irradiation graft polymerization, *Appl. Surf. Sci., 2002,* **200**, 76–93.
11 Q. Zhang, L. Luan, S. Feng, H. Yan and K. Liu, Using a bifunctional polymer for the functionalization of Fe_3O_4 nanoparticles, *React. Funct. Polym.*, 2012, **72**, 198–205.
12 H.M. Yang, C.W. Park, T. Ahn, B. Jung, B.K. Seo, J.H. Park and J.D. Kim, A direct surface modification of iron oxide nanoparticles with various poly(amino acid)s for use as magnetic resonance probes, *J. Colloid Interface Sci.*, 2013, **391**, 158–167.
13 L. Yu, W. Xue, L. Cui, W. Xing, X. Cao and H. Li, Use of hydroxy - propyl-β-cyclodextrin/polyethylene glycol 400, modified Fe_3O_4 nanoparticles for congo red removal, *Int. J. Biol. Macromol.*, 2014, **64**, 233–239.
14 H. Cui, D. Li and Z. Zhang, Preparation and characterization of Fe_3O_4 magnetic nanoparticles modified by perfluoropolyether carboxylic acid surfactant, *Mater. Lett.*, 2015, **143**, 38–40.
15 W. Wang, Y. Jing, S. He, J. P. Wang and J. P. Zhai, Surface modification and bioconjugation of FeCo magnetic nanoparticles with proteins, *Colloids Surf. B*, 2014, **117**, 449–456.
16 M. Ziegler-Borowska, D. Chełminiak, T. Siódmiak, A. Sikora, M.P. Marszałł and H. Kaczmare, Synthesis of new chitosan coated magnetic nanoparticles with surface modified with long-distanced amino groups as a support for bioligands binding, *Mater. Lett.*, 2014, **132**, 63–65.
17 M. Ziegler-Borowska, T. Siódmiak, D. Chełminiak, A. Cyganiuk and M. P. Marszałł, Magnetic nanoparticles with surfaces modified with chitosan–poly [N-benzyl-2-(methacryloxy)-N,N-dimethylethanaminium bromide] for lipase immobilization, *Appl. Surf. Sci.*, 2014, **288**, 641–648.
18 Y. Ding, S.Z. Shen, H. Sun, K. Sun, F. Liu, Y. Qi and J. Yan, Design and construction of polymerized-chitosan coated Fe_3O_4 magnetic nanoparticles and its application for hydrophobic drug delivery, *Mater. Sci. Eng. C*, 2015, **48**, 487–498.
19 P.B. Shete, R.M. Patil, B.M. Tiwale and S.H. Pawar, Water dispersible oleic acid-coated Fe_3O_4 nanoparticles for biomedical applications, *J. Magn. Magn. Mater.*, 2015, **377**, 406–410.
20 X. Zhang, L. Xue, J. Wang, Q. Liu, J. Liu, Z. Gao and W. Yang, Effects of surface modification on the properties of magnetic nanoparticles / PLA composite drug carriers and *in vitro* controlled release study, *Colloids Surf. A*, 2013, **431**, 80–86.

21 P. Tancredi, S. Botasini, O. Moscoso-Londono, E. Méndez and L. Socolovsky, Polymer-assisted size control of water-dispersible iron oxide nanoparticles in range between 15 and 100 nm, *Colloids Surf. A*, 2015, **464**, 46–51.

22 E. Murugan and J.N. Jebaranjitham, Dendrimer grafted core-shell Fe_3O_4–polymer magnetic nanocomposites stabilized with AuNPs for enhanced catalytic degradation of Rhodamine B – A kinetic study, *Chem. Eng. J.*, 2015, **259**, 266–276.

23 M. Chen, L. Wang, J. Han, J. Zhang, Z. Li and D. Qian, Preparation and study of polyacryamide-stabilized silver nanoparticles through a one-pot process, *J. Phys. Chem. B*, 2006, **110**, 11224–11231.

24 A. Chatterjee and S. Mishra, Novel synthesis with an atomized microemulsion technique and characterization of nano-calcium carbonate ($CaCO_3$)/poly(methyl methacrylate) core-shell nanoparticles, *Particuology*, 2013, **11**, 760–767.

25 R. Joksimovic, S. Prévost, R. Schweins, M.S. Appavou and M. Gradzielski, Interactions of silica nanoparticles with poly(ethylene oxide) and poly(acrylic acid): effect of the polymer molecular weight and of the surface charge, *J. Colloid Interface Sci.*, 2013, **394**, 85–93.

26 A. Fedorczyka, J. Ratajczakb, A. Czerwinski and M. Skompska, Selective deposition of gold nanoparticles on the top or inside a thin conducting polymer film, by combination of electroless deposition and electrochemical reduction, *Electrochim. Acta*, 2014, **122**, 267–274.

27 T. Banert and U.A. Peuker, Preparation of highly filled super-paramagnetic PMMA-magnetite nano composites using the solution method, *J. Mater. Sci.*, 2006, **41**, 3051–3056.

28 L.Yu, L. Zheng and J. Yang, Study of preparation and properties on magnetization and stability for ferromagnetic fluids, *Mater. Chem. Phys.*, 2000, **66**, 6–9.

29 A. Cosultchi, J.A. Ascencio-Gutierrez, E. Reguera, B. Zeifert and H. Yee-Madeira, On a probable catalytic interaction between magnetite (Fe_3O_4) and petroleum, *Energy Fuels*, 2006, **20**, 1281–1286.

30 T. Madrakian, A. Afkhami, H. Mahmood-Kashani and M. Ahmadi, Superparamagnetic surface molecularly imprinted nanoparticles for sensitive solid-phase extraction of tramadol from urine samples, *Talanta*, 2013, **105**, 255–261.

31 S. Peng, C. Wang, J. Xie and S. Sun, Synthesis and stabilization of monodisperse Fe nanoparticles, *J. Am. Chem. Soc.*, 2006, **128**, 10676–10677.

32 F. Bouyer, A. Robben, W. Yu and M. Borkovec, Aggregation of colloidal particles in the presence of oppositely charged polyelectrolytes: effect of surface charge heterogeneities, *Langmuir*, 2001, **17**, 5225–5231.

33 E. Illés and E. Tombácz, The effect of humic acid adsorption on pH-dependent surface charging and aggregation of magnetite nanoparticles, *J. Colloid Interface Sci.*, 2006, **295**, 115–123.

34 S.A. Gomez-Lopera, J.L. Arias, V. Gallardo and A.V. Delgado, Colloidal stability of magnetite/poly(lactic acid) core/shell nanoparticles, *Langmuir*, 2006, **22**, 2816–2821.